Dynamics of the Mesosphere and Lower Thermosphere Based on Results of Observations on the SURA Facility

N. V. Bakhmetieva[a], *, V. D. Vyakhirev[a], G. I. Grigoriev[a], M. N. Egerev[a], E. E. Kalinina[a], A. V. Tolmacheva[a], I. N. Zhemyakov[a], G. R. Vinogradov[a], and K. M. Yusupov[b]

[a]*Radiophysical Research Institute, Nizhny Novgorod State University N.I. Lobachevsky (NIRFI), Nizhny Novgorod, Russia*
[b]*Kazan (Volga) Federal University, Kazan, Russia*
*e-mail: nv_bakhm@nirfi.unn.ru

Abstract—The results of studies of atmospheric dynamics in the altitude range of 60−130 km are presented based on measurements of the velocity of vertical plasma motion, the temperature and density of the neutral component, and the turbopause height. The measurements were carried via resonant scattering of radio waves by artificial periodic inhomogeneities of the ionospheric plasma. The method is based on ionospheric perturbation by powerful high-frequency radio emission, the creation of periodic inhomogeneities in the field of a standing wave, which forms upon reflection from the ionosphere of a powerful radio wave emitted into the zenith, and the location of inhomogeneities by test radio waves. The parameters of the neutral component, the turbulent velocity, and the height of the turbopause are determined from the relaxation time of the signal scattered by the inhomogeneities after the end of the ionospheric impact. The measurement of the phase of the scattered signal makes it possible to determine the rate of vertical plasma motion. The experiments were carried out on a SURA heating facility (56.15° N; 46.11° E). The paper presents and analyzes the time−altitude dependences of the vertical velocity and temperature, which are largely due to the propagation of atmospheric waves during various natural phenomena. The results of determination of the turbopause height and turbulent velocity are presented.

1. INTRODUCTION

The state of the mesosphere and the lower thermosphere, i.e., the Earth's atmosphere at altitudes of 60−130 km, is largely determined by its temperature and density, composition, electron concentration, horizontal and vertical movements, turbulent phenomena, and wave processes. The physical parameters describing the state of this transition region between the lower and upper atmosphere, which causes thermospheric interaction regulated by solar activity, and the troposphere, which forms the weather and climate, experience variations in time and space. The dynamics of the atmosphere at these altitudes largely determines the overall picture of its state, and allows energy exchange between the mesosphere and the thermosphere. The study of this area of the Earth's atmosphere, its heterogeneous structure and dynamics, and manifestations of wave motions in variations in the characteristics of the ionized and neutral components is an urgent problem of cosmic plasma physics and radio wave propagation.

The characteristics and properties of the mesosphere and the lower thermosphere are significantly affected by turbulence and atmospheric waves, which manifest themselves both in the characteristics of signals scattered by inhomogeneities and in variations in temperature and velocity. It is important to determine the level of turbopause, i.e., the altitude regions in which turbulent mixing is replaced by diffusive gas separation. Above the turbopause the role of ambipolar diffusion in the transfer processes increases; still higher, the role of plasma drift in electric and magnetic fields increases. Turbulent formations can be transported in height by vertical plasma movements and atmospheric waves.

There are more than 100 works on experimental studies of the dynamics of the ionosphere at mesospheric-thermospheric heights conducted with different study methods. Here, we give only a few publications covering various aspects of experimental and theoretical research in this direction (Danilov et. al., 1979; Hananyang, 1985; Kalgin and Danilov, 1993; Hocking, 1996; Kirkwood, 1996; Fritts and Alexander, 2003; Offermann et. al., 2006; Somsikov, 2011; Karpov and Kshevetsky, 2014; Perminov et al., 2014; Karpov et al., 2016; Vlasov and Kelley, 2014; Medvedeva and Ratovsky, 2017). The modernization of measuring equipment and the development of new measurement

methods stimulate studies of atmospheric dynamics. One method to obtain data on the time–altitude variations of the parameters of the neutral component uses ionospheric perturbations by the powerful radio emission of a heating facility to determine the characteristics of a regular, i.e., natural, wave propagation medium.

The goal of this work is to study the dynamics of the Earth's lower ionosphere based on measurements of the time-altitude characteristics of signals scattered by artificial periodic inhomogeneities (APIs) of the ionospheric plasma generated by reflection from the ionosphere of high-power high-frequency radio emission from the SURA heating facility (56.15° N; 46.11° E), which in turn, allows one to study variations in the temperature and density of the neutral component, and the velocity of the vertical regular and turbulent motions of the medium to determine the turbopause height and to study the effect of atmospheric waves on the change in these parameters. The work mainly presents the results of experiments performed at the SURA stand in 2010−2018. Some previous results taken from publications cited in the article are used.

2. RESEARCH METHOD OF ATMOSPHERIC DYNAMICS

The parameters of the neutral component and the vertical velocity of the plasma in the altitude range 60−120 km were determined via resonance scattering of radio waves by artificial periodic inhomogeneities of the ionospheric plasma (Belikovich et al., 1999, 2006; Bakhmeteva et al., 1996a, 1996b, 2002, 2005, 2010a, 2010b; Belikovich et al., 2002; Bakhmetieva et al., 2016, 2017a, 2017b, 2018; Tolmacheva et al., 2013, 2015). These works provide a detailed description of the API technique and methods to determine the characteristics of the ionosphere and neutral atmosphere. The method is based on the creation of periodic irregularities when a powerful radio wave is reflected from the ionosphere with the formation of a quasi-periodic structure of temperature and electron concentration due to uneven heating of the ionospheric plasma. At the antinodes of the standing wave, the electron gas is heated, resulting in a periodic structure with a spatial period Λ equal to half of the length λ of the powerful radio waves in the plasma. Due to excess pressure, the plasma is pushed into the nodes of the standing wave upon the formation of electron-concentration inhomogeneities (Belikovich et al., 1999; Belikovich et al., 2002; Kagan et al., 2002). The irregularities scatter the probe radio waves, and, when the Bragg scattering condition is fulfilled, the receiving unit receives a signal, the intensity of which is due to the in-phase addition of the waves scattered by each inhomogeneity. The scattering of probe radio waves by these irregularities has resonance properties, i.e., the received signal has a significant amplitude with equal frequencies and polarizations of the powerful and probe radio waves. The last condition is one of two methods for the diagnosis of irregularities (Belikovich et al., 1999; Beliko-vich et al., 2002).

The times of the development of irregularities and their disappearance (relaxation) after the end of heating are determined by the composition, the density and temperature of the atmosphere, and the degree of dissociation and ionization, which allows the use of a method based on the creation of an API to diagnose the ionosphere and neutral atmosphere. In the D region, the main role in API formation is played by the temperature dependence of the electron attachment coefficient to neutral molecules. In the E layer, it is played by the diffusion redistribution of plasma under the influence of excess pressure of the electron gas, and, lastly, plasma in the F region is redistributed under the influence of striction force (Belikovich et al., 1999; Belikovich et al., 2002). After heating in the E layer, irregularities relaxation occurs under the influence of ambipolar diffusion and due to the temperature dependence of the coefficients of electron detachment in the D region. The measurement of the phase of the scattered signal makes it possible to determine the rate of vertical plasma motion, which is equal to the velocity of the neutral component at the heights of the mesosphere−lower thermosphere (Gershman, 1974).

For transmitter frequencies of 4-6 MHz for the SURA facility with an effective radiated power of the facility on the order of 80−120 MW used in these experiments, the relative perturbation of the concentration in the irregulaties can be $\Delta N/N \approx 10^{-4}-10^{-3}$ in the E layer and $\Delta N/N \approx 10^{-3}-10^{-2}$ in the D region. The first experiments showed that the $\Delta N/N$ in-phase addition of signals scattered by each irregularity at such values provides a signal-to-noise ratio of ~10−100 in the E layer and is usually slightly smaller in the D region. Pulsed radio sounding of the perturbed region is used for the location of periodic irregularities and registration of the signal scattered by them after the facility stops at the stage of inhomogeneity relaxation. The amplitude is calculated from digital recordings of the quadrature components of the scattered signal with a pitch of 0.7−1.4 km and a time resolution of 15 s at each height A and phase φ of the scattered signal, the time dependences of which are then approximated by linear functions of the form $\ln A(t) = \ln A_0 - t/\tau$; $\varphi(t) = \varphi_0 + 4\pi V t/\lambda$. The API relaxation time (the relaxation time of a signal scattered by inhomogeneities) τ is determined by the decay of the signal amplitude in e times, and the velocity V of the vertical plasma motion is determined according to the change in the phase φ in time. With the indicated definition of velocity, its positive values correspond to a downward movement. At heights without atmospheric turbulence, the relaxation of irregularities in E regions due to ambipolar diffusion with characteristic time is
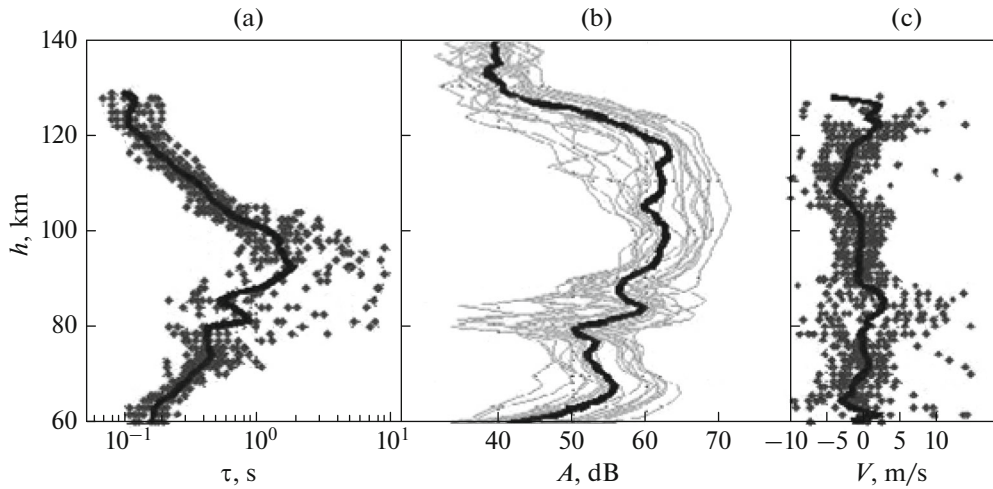
Fig. 1. Altitude profiles of scattered signal characteristics on September 30, 2016: (a) relaxation times τ; (b) amplitude A, and (c) vertical velocity of the plasma V for the observation session of 1354–1358. The curves correspond to characteristics averaged over 5 min at each height.

$\tau = \dfrac{1}{K^2 D} = \dfrac{M_i \nu_{im}}{k_B(T_{e0} + T_{i0})K^2}$, where k_B is the Boltzmann constant, $K = 4\pi/\lambda$ is the wavenumber of a standing wave, $\lambda = \lambda_0/n$ is the wavelength in the medium, n is the refractive index, D is the coefficient of ambipolar diffusion, M_i is the molecular mass of ions, T_{e0} and T_{i0} are the unperturbed values of electron and ion temperatures, and ν_{im} is the frequency of collisions of ions with neutral molecules. The methods to determine the electron concentration N, the temperature T and density ρ of the neutral component, the turbulent velocity, and the masses of the main ions in the sporadic E layer are based on the expression above for τ (Belikovich et al., 1999; Bakhmeteva et al., 2005, 2010; Belikovich et al., 2002). In the absence of a sporadic E layer (the E_s layer) and turbulence, the height dependence of the relaxation time of the API τ (h) corresponds to the diffusion approximation. The turbulent velocity and height of the turbopause are determined from the diffusion law by the deviation τ (h) (Belikovich et al., 2002; Bakhmetieva et al., 2018).

Figure 1 gives an example of altitude profiles of the scattered signal characteristics on September 30, 2016: (a) relaxation time τ; (b) amplitude A; and (c) the vertical velocity of the plasma V for the observation session 1354–1358. The curves correspond to characteristics averaged over 5 min at each height. In this example, the diffusion law of relaxation corresponds to a height interval of $\sim$100–120 km. The relaxation times are in good agreement with the diffusion dependence $\tau(h)$. Below 100 km, atmospheric turbulence begins to have an effect, while the relaxation time of the scattered signal decreases. At an altitude of 85 km, a local increase in the amplitude of the scattered signal is ensured by an anomalously low sporadic E layer. A local maximum of the relaxation time is observed at the same height. For the heights of D regions, the amplitude and relaxation time change with height in full accordance with the temperature dependence of the electron detachment coefficient (Belikovich et al., 1999, 2002). In the example in Fig. 1c, the direction of vertical movement velocity is constantly changing for 5 min, and negative V values (upward movements) are replaced by positive (downward values) at an altitude of $\sim$85 km. The velocity values mainly cover the range of values from -5 m/s to $+5$ m/s. Figure 2 shows the time dependence of the scattered signal relaxation at three heights on September 28, 2018 (a) and on September 27, 2018 (b): circles—height 100 km, points—height 105 km, and triangles—height 112 km. Wave variations τ (t) are clearly visible with a period of 15 min to 1 h or more. The sharp increase in the relaxation time of about 13 h is due to the appearance of a sporadic E layer, which formed directly above the observation point and was recorded by the ionosonde.

When the heating facility is switched off, the periodic structure below the turbopause level is destroyed by both ambipolar and turbulent diffusion, as a result of which the process of relaxation of inhomogeneities is faster and the relaxation time of the scattered signal decreases as compared to diffusion time. The process of the influence of atmospheric turbulence on the relaxation time of the scattered signal is shown in Fig. 1. It can be seen that turbulence begins to affect the API below 100 km, and the turbopause level is located in the altitude range 95–100 km. The relaxation times are in good agreement with the diffusion dependence $\tau(h)$, but they noticeably deviate from it below the turbopause h_t under the influence of turbulence.

The problem of the influence of atmospheric turbulence on the amplitude and relaxation time of a scattered signal has been studied in detail (Belikovich and
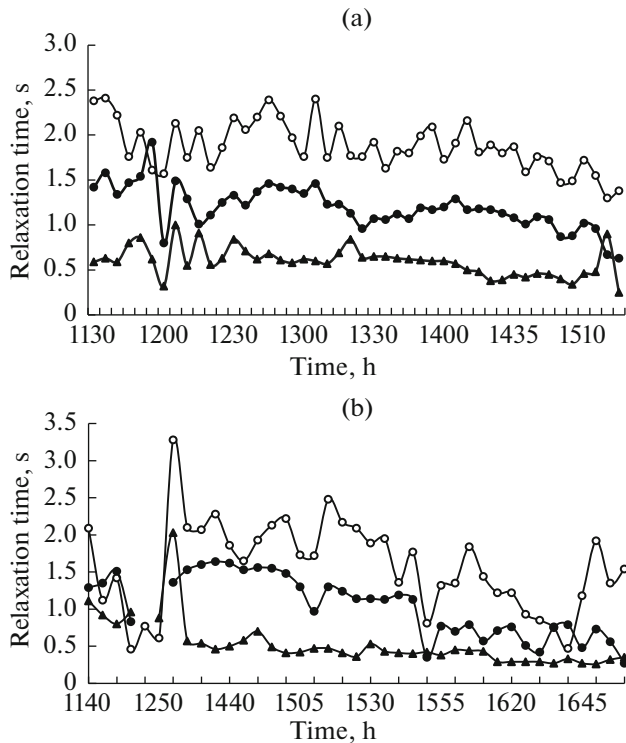
Fig. 2. Dependence of the relaxation time of the scattered signal on time at three heights for (*a*) September 28, 2018, and (b) September 27, 2018: circles—height of 100 km, points—height of 105 km, triangles—height of 112 km. Wave movements with a period of 15 min to 1 h or more are clearly visible.

Benediktov, 1995; Belikovich et al., 1999; Belikovich et al., 2002). Under the assumption that distortions of the periodic structure are created only by the field of the vertical component of turbulent velocity and that the scattering volume is much larger than the period of the irregular structure, which is equal to half the length of the heating wave, an expression was obtained (Belikovich and Benediktov, 1995; Belikovich et al., 1999; Belikovich et al., 2002) for the velocity of turbulent motion V_t as a function of the experimentally measured and diffusion relaxation times of the API. The error in this method to determine the turbulent velocity does not exceed several cm/s.

3. IONOSPHERE DURING OBSERVATIONS

Experiments on the study of the ionosphere by the API method were carried out during years of high and low solar activity; with geomagnetic disturbances and in calm conditions; under the conditions of the propagation of moving ionospheric disturbances and atmospheric waves; with developed turbulence; with the existence of translucent and shielding sporadic *E* layers; in the sunset-sunrise period; in conditions of solar eclipses; and at the equinox (Belikovich et al., 1999; Bakhmeteva et al., 2005, 2010a, 2016, 2017; Tol-

macheva and others 2013, 2015; Belikovich et al., 2002; Bakhmetieva et al., 2017; Bakhmetieva et al., 2018). This paper presents the results obtained mainly in experiments in 2010−2018. These years fell in the 24th cycle of solar activity with maximum activity in 2014−2015 and an average Wolf number, which is equal to the individual months of these years, of ∼100−120. In other years, experiments were conducted against the background of growth and decline, as well as during periods of minimum solar activity with a Wolf number of about 10. The time of observation sometimes coincided with periods of increased geomagnetic activity. Thus, during experiments on the diagnosis of the lower ionosphere in March 2015, a strong geomagnetic storm was observed on the night of March 17−18. The index of geomagnetic activity in these hours at the latitude of the SURA facility reached 6−8 points, which corresponds to the level of a rigid geomagnetic storm, and an aurora was observed above the location where the SURA facility is located. A partial solar eclipse with a maximum phase of 0.586 occurred on March 20, 2015, while the geomagnetic field was already calm or slightly perturbed. At sunset and sunrise hours on August 12−13, 2015, during ionospheric observation by the API method with relatively high solar activity, the geomagnetic field was calm with $Kp = 2−3$. During the daytime hours on September 26−28, 2016, the geomagnetic disturbance intensified at night from $Kp = 3−4$ to $Kp = 6$, but no observations were made at this time. On observation days in September and October of 2017 and 2018 no geomagnetic disturbances were recorded at minimal solar activity. Thus, the bulk of the results of measurements of the parameters of the neutral component and vertical velocity presented in the work were obtained under calm and slightly disturbed ionospheric conditions during years of minimal, high, and average solar activity.

For the formation of artificial periodic irregularities, a powerful radio wave must be reflected from the ionosphere. When frequencies of 4.7−5.6 MHz were used to create periodic inhomogeneities, this condition was almost always fulfilled, except for night conditions with low solar activity and in the winter months. During observations, especially from May to September, shielding and translucent sporadic *E* layers were often observed, with the critical frequencies sometimes reaching 9−10 MHz. Shielding layers with a high critical frequency lead to an increase in the amplitude of the standing wave, in the field of which inhomogeneities form and thereby improve the conditions for the reception of the signal scattered by them in the *D* region, relatively high layers located above 120 km, and in the *E* layer. In addition, as follows from the expression for the relaxation time of inhomogeneities, τ is proportional to the mass of ions. This makes it possible to estimate the mass, i.e., to determine the type of predominant metal ions in the E_s layer (Kagan et al., 2002; Bakhmeteva et al., 2010a).

4. TIME–ALTITUDE VARIATION IN THE VERTICAL PLASMA VELOCITY

Vertical movements are one of the components of the general circulation of the atmosphere. To date, this type of atmospheric motion remains the least studied. The results of long-term measurements of the vertical movement velocity based on the creation of an API were summarized by Belikovich et al. (1999, 2002). These include studies from the 1980s and 1990s. The seasonal–daily variations of the vertical velocity were studied in experiments in 1990–1992; the seasonal variation of the average daily and monthly average V values was obtained at altitudes of 97–117 km. The nature of seasonal–daily variations in velocity was revealed to be complex: upward movements dominated above 90 km (up to 70% of all data). The average monthly velocity values were about 1 m/s at altitudes below 100 km, increasing to 5 m/s with increasing altitude. The results of the study of vertical movements in different environmental conditions are also contained in works by Bakhmeteva et al. (1996b, 2010a, 2016, 2017). Note that existing models of the circulation of the middle atmosphere give average values of the velocities of vertical movements up to several cm/s at heights of 80–100 km (*Izmerenie ...*, 1978; Karimov, 1983). The digital registration of quadrature components of the scattered signal makes it possible to register fast fluctuations of the vertical velocity. The main features of velocity variations in the lower ionosphere are rapid temporal variations, i.e., a change in the magnitude and often the velocity direction, for 15 s, i.e., during one measurement; high velocity values reaching 10 m/s during one measurement; velocity values averaged over a 5-min time interval that usually range from −5 m/s to +5 m/s; and relatively large values of the vertical velocity due to wave motions in the atmosphere. In the time dependence of the vertical velocity, wave motions appear with a period of 5–10 min to 4–5 h, and the wave period in height is 5–25 km (Bakhmeteva et al., 1996b, 2010a, 2016, 2017; Belikovich et al., 1999; Belikovich et al., 2002; Bakhmet'eva et al., 2018).

A few examples of altitude–time variations in vertical velocity are presented here. Figures 3a and 3b show the vertical altitude profiles V and amplitudes of the scattered signal A for two measurement sessions on August 9, 2017. The dotted curves correspond to characteristics averaged over 5 min at each height. At altitudes of 90–100 km, an increase in the amplitude of the scattered signal and its amplitude is due to the existence of a sporadic E layer with an increased electron concentration of its relative background value in E regions. At the same altitudes, there is a change in the direction of velocity, and its transition through a zero value. In most cases, the change in the velocity direction, during which the upward movement is replaced by a downward movement at a given height, corresponds to the height of the maximum of the sporadic E layer, which indicates that the E_s layer forms immediately above the observation point as a result of the redistribution of charged particles in the Earth's magnetic field (wind-shear theory) (Gershman, 1974; Gershman et al., 1976; Whitehead, 1961; Mathews, 1998). If we follow wind-shear theory, according to which the sporadic E layer, i.e., an ionization layer with an increased electron concentration relative to the background E region, formed due to the redistribution of metal ions in an inhomogeneous velocity field in the presence of a magnetic field, then the velocity at the height of the E_s layer should take a zero value or have a gradient of the desired direction for the "dropping" of ions, and, behind them, electrons into thin plasma layers. This was the case in most of our observations of the E_s layer (Bakhmeteva et al., 2005, 2010a).

Figure 3c shows the altitude velocity profiles obtained on September 28, 2018, for the hourly observation interval from 1300 to 1400. The profiles are plotted with an interval of 5 min. The boundaries from −10 m/s to +10 m/s correspond to each pair of vertical lines, and the vertical line passing between them corresponds to a zero value of velocity. Figure 3c shows a constant change in the velocity direction, as well as deeper variations in the D region and at the bottom of the E layer above 85 km. The altitude region above 85 km is characterized by the development of atmospheric turbulence. The lack of data in the altitude range 76–85 km is due to an increase in the atomic oxygen content, which prevents API formation in the D region (Belikovich et al., 1999; Belikovich et al., 2002).

Figure 4a shows the dependence of the vertical plasma velocity on September 28, 2018 averaged over 5 min for three heights of the D region: 28–66 km, 76 km, and 85 km, and Fig. 4b shows the dependence for three E-layer heights: 100 km, 105 km, and 112 km. The range of velocity variations ranged from −6 to +6 m/s in the D region and from −3 to +3.5 m/s in he E layer. Wave-like velocity variations are visible with a constant change of direction and a period of 5 min to 1 h in the D region and up to 3 h in the E layer, which indicates an intense dynamics of the studied region of heights.

Variations in the vertical velocity over time are due to a number of reasons, one of which is the constant existence in the lower ionosphere of wave processes of various natures, including internal gravitational waves (IGWs) and tides. Figure 4b shows the range of velocity fluctuations and the period of increasing wave motions with height. The same features are reflected in Figs. 5a, 5b, and 5c, which show the changes in velocity over time in the evening hours of August 12, 2015. The dashed lines in the figures show the velocity values smoothed by the moving average over five points illustrating its growth with height with a change in the maximum period of variations from 25–30 min at an altitude of 100 km before ∼100 min at an altitude
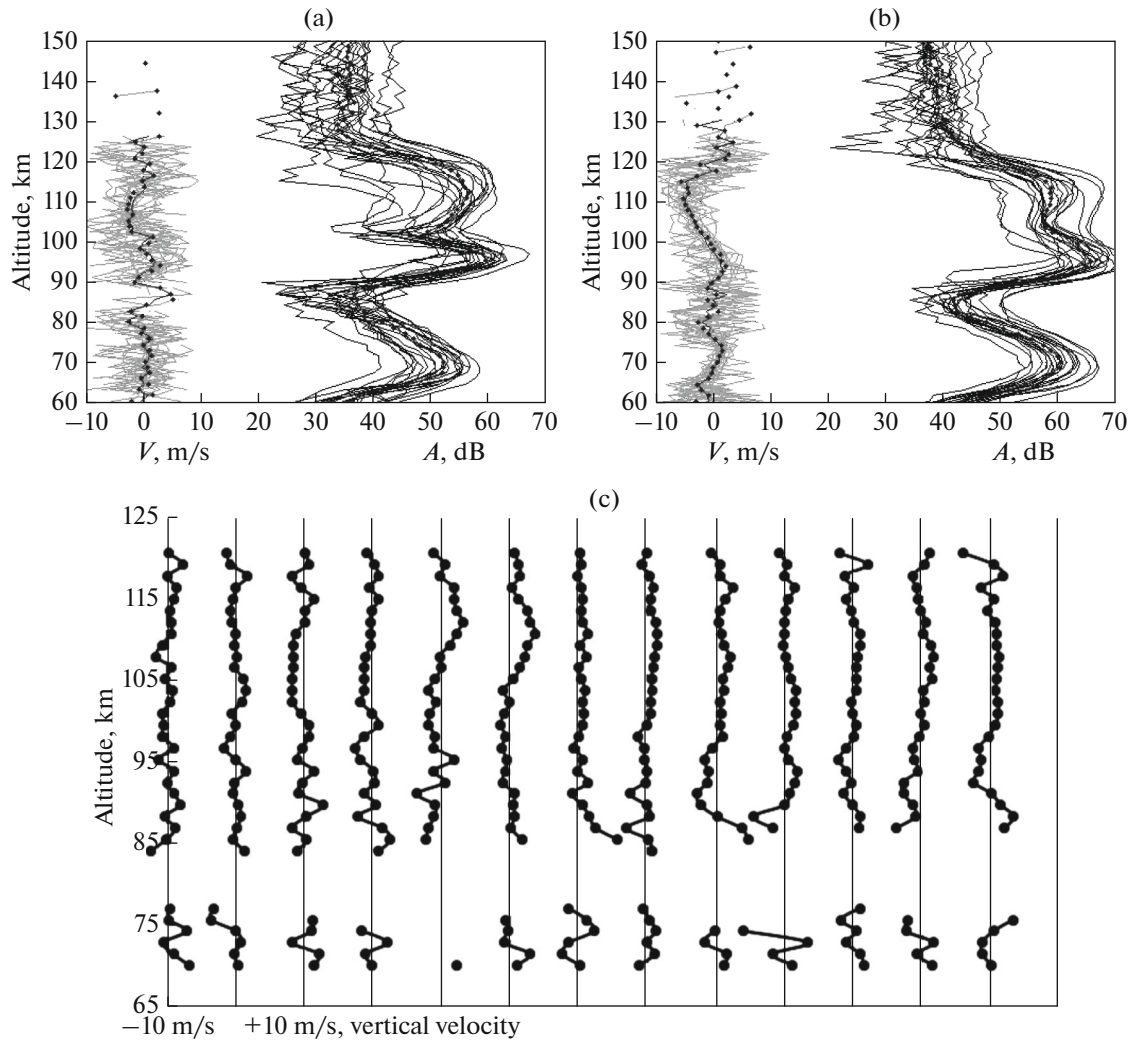
Fig. 3. Altitude profiles of vertical plasma velocity V and amplitudes of the scattered signal A for two 5-min measurement sessions on August 9, 2017, (a) at 1800 and (b) 1840. The curves with dots correspond to characteristics averaged over 5 min at each height. (c) Successive vertical altitude profiles of the vertical plasma velocity on September 28, 2018, for the hourly observation interval from 1300 to 1400. Profiles are built with an interval of 5 min. The boundaries of the velocity change from -10 m/s to $+10$ m/s, and the vertical lines pass through the zero velocity.

of 105 km and up ~2.5 h at an altitude of 112 km. The most noticeable wave manifestations in velocity variation were observed during solar eclipses and during the sunset and sunrise. They are due to the transition to the twilight or night (depending on the eclipse phase) ionosphere mode and the passage of the terminator through the observation point. Figure 6 shows the vertical plasma motion velocity during a single solar eclipse on March 20, 2015, at three altitudes; the points correspond to the velocity values at an altitude of 100 km, the circles indicate an altitude of 110 km, and the triangles denote an altitude of 115 km. The eclipse phases—initial, maximum, and final—are shown by vertical lines. Each point corresponds to a 5-min averaging of velocity values. Common to Figs. 5 and 6 are increasing velocity variations upon the approach of the maximum eclipse phase

and in the pre-entry period and an increase in the period of variations.

5. VARIATIONS IN NEUTRAL COMPONENT PARAMETERS

In accordance with the algorithm for the processing of the amplitude of the scattered signal described in Section 2, the temperature and density of the neutral component were obtained in the altitude range of $90-120$ km, and the turbopause level was determined. We give and discuss several examples of their time–altitude variations.

### 5.1. Temperature and Density of the Neutral Atmosphere

As noted above, the basis for the determination of the parameters of the neutral atmosphere, i.e., the

(a)

(b)
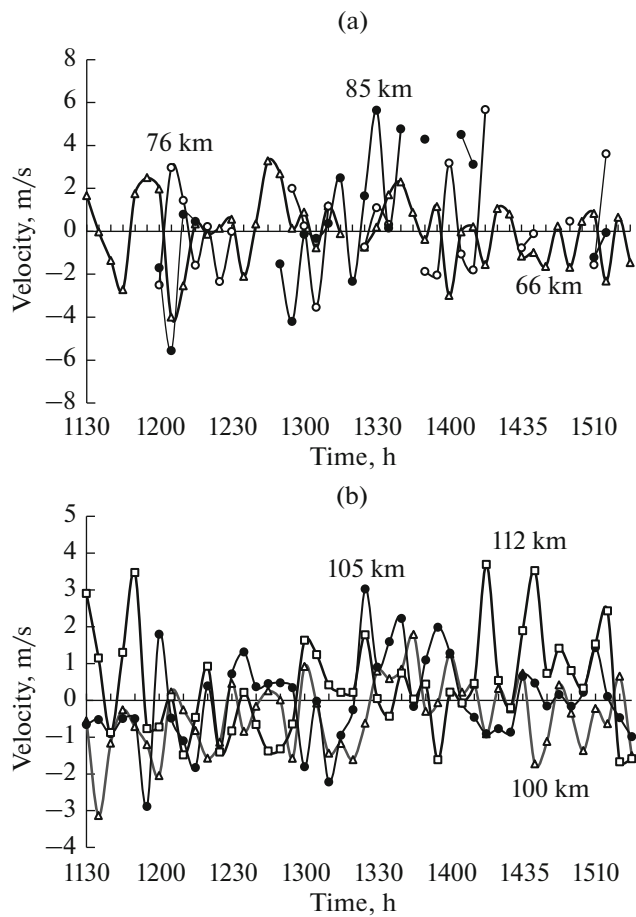
Fig. 4. Dependence of the values of the velocity of vertical plasma motion averaged over 5 min on September 28, 2018, for (a) three heights of the D regions (66 km, 76 km, and 85 km) and (b) three heights of the E layer (100 km, 105 km, and 112 km). Wave motions with a period of 5 min to 1 h are clearly visible in Fig. 4a and a period up to 3 h are visible in Fig. 4b.

temperature and density of the neutral component in the lower part of the E layer at altitudes of 90−120 km, is the experimentally obtained altitudinal dependence of the relaxation time $\tau(h)$ of a signal scattered by periodic irregularities (Belikovich et al., 1999; Belikovich et al., 2002). The results of the determination of the temperature under different ionospheric conditions were given in the literature (Belikovich et al., 1999; Bakhmeteva et al., 2010b; Tolmacheva et al., 2013; Bakhmet'eva et al., 2013; Tolmacheva et al., 2015). This section discusses several examples of the determination of the temperature and density obtained mainly in recent experiments in 2016−2018.

In Figure 2b, which gives an example of the dependence of the relaxation time τ of a scattered signal at three effective heights on September 27, 2018, the relaxation time is subject to oscillations with different periods. Since the height dependence $\tau(h)$ the parameters of the neutral component are determined, similar

(a)

(b)

(c)
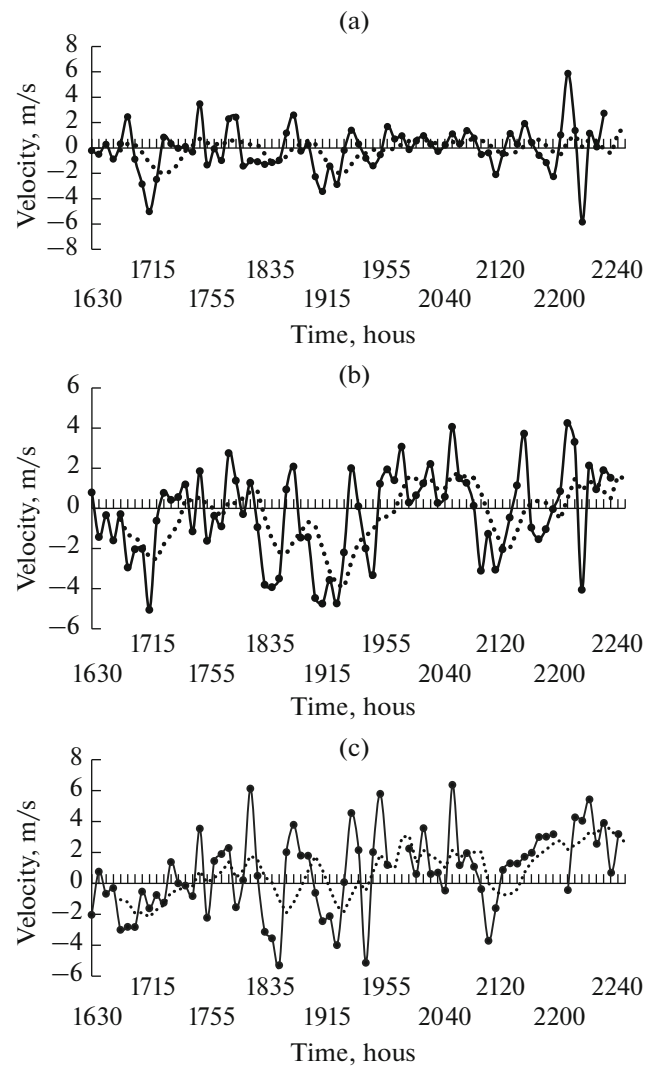
Fig. 5. Changes in velocity over time in the evening hours of August 12, 2015: (a) height of 100 km, (b) height of 105 km, and (c) height of 112 km. The dotted lines in the figures show the velocity values smoothed by the five-point moving average method, which demonstrate an increase in velocity with height with a change in the maximum period of its variations from 25−30 min at an altitude of 100 km, up to 100 min per 105 km, and up to 220 min per 112 km.

patterns should be expected in the time−altitude changes in temperature and density. Figure 7a presents the time dependences of the temperature of the neutral component for three heights on September 27, 2018, over a 5-min interval of averaged relaxation times. It can be seen that the deepest temperature variations occur at an altitude of 100 km. The highest T values were obtained, sometimes reaching 300 K. These features can be explained if we take into account that the altitude of 100 km is already very close to the turbulent region, where the error in the determination of atmospheric parameters increases. However, temperature values of 50 K, which are uncharacteristic for these altitudes, are not yet clear. The largest number of tem-
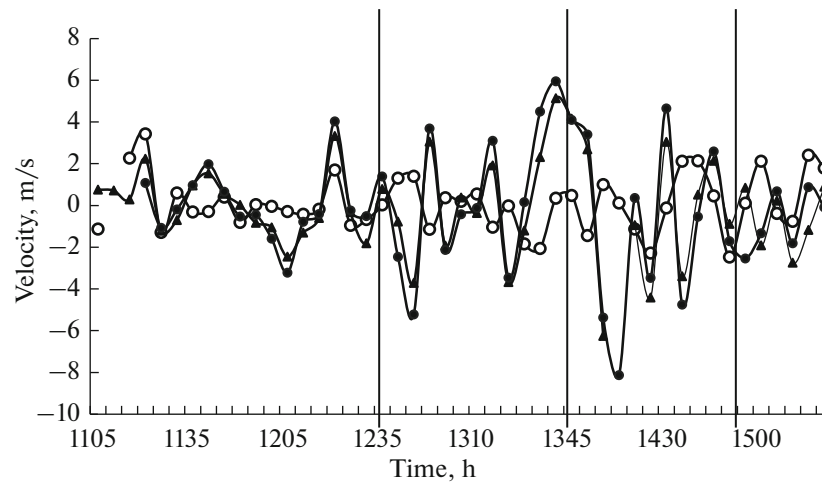
Fig. 6. Rate of vertical plasma motion during a single solar eclipse on March 20, 2015, at three altitudes: points—velocity values at an altitude of 100 km, circles—altitude of 110 km, triangles—altitude of 115 km. The eclipse phases—initial, maximum, and final—are shown by the vertical lines.

perature data was obtained for an altitude of 105 km. One can see, in particular, temperature fluctuations with a range of up to 10−100 K in neighboring 5-min averaging cycles. A limited number of temperature values were obtained at an altitude of 112 km, which is associated in this particular case with a more frequent violation of the diffusion approximation of the relaxation time at this altitude as compared to lower altitudes. These features of the time−altitude temperature variations are undoubtedly associated with intense dynamic processes in the lower thermosphere, the nature of which is not always obvious.

Figure 7b presents the dependences of the temperature of the neutral component in the daytime at an altitude of 100 km for September 26, 2016, and September 28, 2017. Measurements on these days were carried out in a similar ionospheric and calm geomagnetic situation. The intervals of temperature changes are typical at these altitudes. For these days, there is a general similarity between temporary variations with pronounced periods from 15 min to 1.5 h.

Noticeable wave perturbations of the neutral component in the lower part of E regions were manifested in ionospheric observations by the API method during solar eclipses and at sunset−sunrise hours. Figure 8a gives the dependences of temperature and neutral density on time during a single solar eclipse on March 20, 2015, with a maximum phase of 0.586. Vertical lines indicate the initial, maximum, and final eclipse phases. By the maximum eclipse phase, the temperature decreased on average by 100 K, experiencing strong variation and recovering to the previous values by the end of the eclipse. Comparing these variations with temporary changes in the velocity of vertical movement shown in Fig. 6, as well as with changes in the electron concentration presented by Bakhmeteva et al. (2017, 2017a), we conclude that there is a signifi-

cant change during the eclipse of both the ionized and neutral components of the atmosphere at these altitudes. We also note a high correlation of changes in neutral temperature and density. Intense manifestations of wave motions in the parameters of the neutral component are shown in Fig. 8b, which refers to the period of sunrise on June 13, 2015. It is reasonable to assume that these manifestations are provided by the passage of the terminator through the observation point.

The periods of waves contributing to variations in atmospheric parameters correspond to internal gravitational waves (Hines, 1975; Karimov, 1983; Brunelli and Namgaladze, 1988; Grigoriev, 1999; Fritts and Alexander, 2003; Somsikov, 2011; Karpov et al., 2016; Borchevkina and Karpov, 2018). The developed dynamics of the lower thermosphere and the differences in changes in temperature and density at different heights are illustrated Fig. 9, in which their variations are presented on September 28, 2018, at altitudes of 100 km and 105 km. Pronounced wave movements with a period of 15 min to 2 h or more are clearly visible, having a complex picture of temporary temperature variations with a range of fluctuations from ∼10−15 to ∼100 K. The temperature averages ∼170 K over the entire observation period and differs little at both heights. However, significant differences in the nature of temporary changes in temperature and density at heights of 100 and 105 km are also visible. Thus, at an altitude of 105 km after 13 h, there were short, 10-min oscillations with a range of up to 40 K against the background of longer-period waves with a period ∼80 min. At the same time, the minimum range of temperature fluctuations at an altitude of 100 km is ∼20 K with a 15-min period and is accompanied by the manifestation of wave movements with a swing of ∼100 K and a
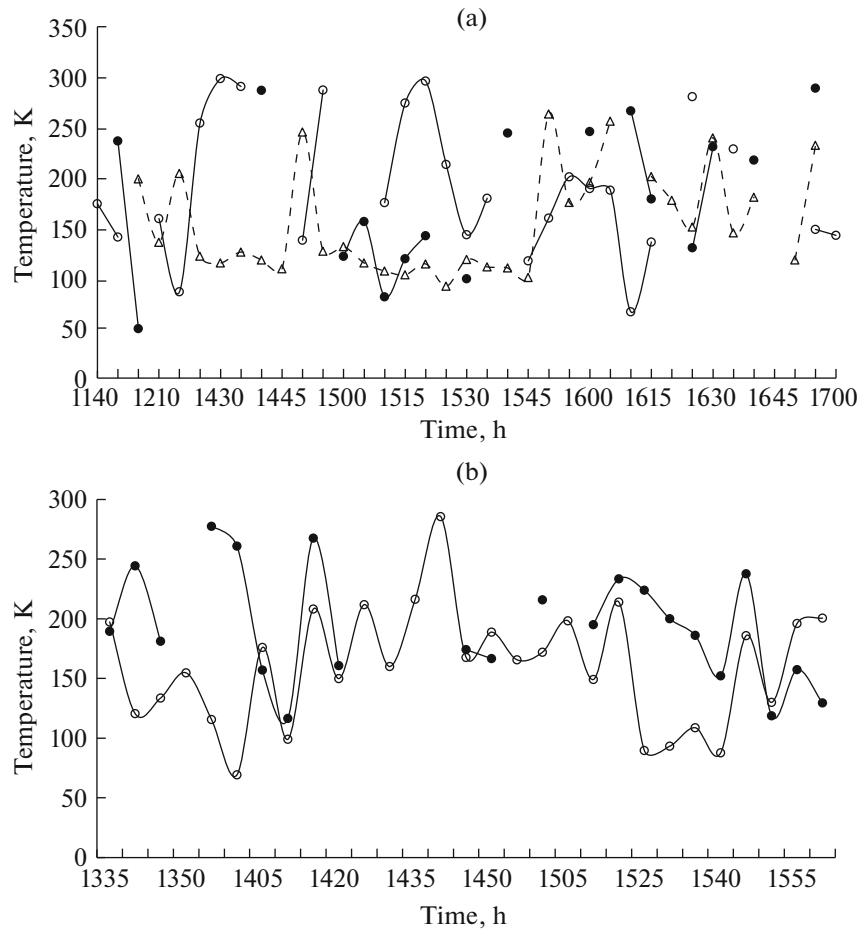
Fig. 7. Dependence of (a) of the time of the neutral component averaged over an interval of 5 min on September 27, 2017, at three heights 100 km (circles), 105 km (triangles) and 112 km (points) and (b) of the temperature of the neutral component at an altitude of 100 km on September 26, 2016 (points), and September 28, 2017 (circles).

period of ~25–30 min and large-scale oscillations of ~150 K and a period of about 1.5 h.

The relationship between temperature variations, vertical velocity, and the effect of atmospheric waves and medium instabilities on them has been discussed (Bakhmeteva et al., 2010b, 2017; Tolmacheva et al., 2013; Tolmacheva et al., 2015). Figure 10 gives two examples of altitude profiles of temperature and vertical velocity averaged over 5 min that change "in phase" (September 2010), i.e., when the temperature and velocity modulus simultaneously increase over the entire altitude range (Fig. 10a) and both the maximum and temperature values are reached at the same heights as the values of the velocity modulus, and "in antiphase" (September 2014), when the local maximum of the temperature falls at heights with local minima of the velocity modulus for almost the entire height range (Fig. 10b) The altitudinal range of temperature and velocity variations was 5–20 km. Similar velocity profiles were considered in detail (Bahmeteva et al., 2010b, 2017; Tolmacheva et al., 2013; Tolmacheva et al., 2015). Tolmacheva et al. (2013) and

Bakhmetieva et al. (2016) presented and discussed examples of experimental altitudinal temperature profiles $T(h)$ with a negative altitudinal gradient and the subsequent development of perturbations of atmospheric parameters. Tolmacheva et al. (2013) showed that an important role in temperature variations of the neutral component is played by the instability of the medium, which is associated with its significant decrease with height. In the approximation of the linear altitude dependence of temperature, a sufficient condition for the development of instability is the fulfillment of the condition $dT/dh < -(10-12 \text{ K/km})$. The excitation of IGWs of various periods and the associated instabilities should lead to turbulization of the medium. We have found that there may be significant turbulent velocities up to 5–7 m/s in an atmosphere perturbed by waves below the turbopause height. Based on the analysis of a large volume of the time–altitude dependences of temperature and velocity, it was concluded (Tolmacheva et al., 2013) that convective instabilities can be observed when an IGW propagates above 100 km, which ensures energy trans-
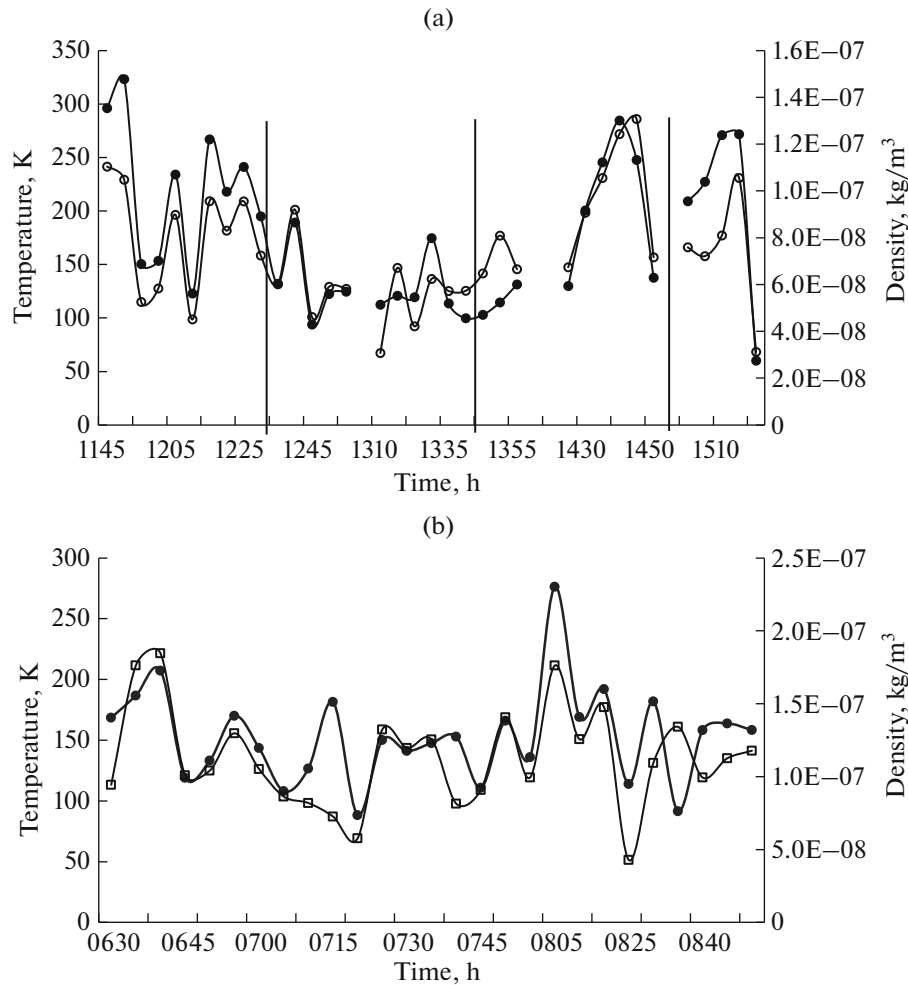
Fig. 8. Temperature (circles) and density (points) of the neutral component at an altitude of 100 km during a single solar eclipse on March 20, 2015. (a) The eclipse phases are shown by vertical lines, and the temperature (points) and density (circles) of the neutral component are shown for the altitude of 105 km after sunrise on June 13, 2015. The averaging interval was 5 min.

fer from the turbulent region to the lower thermosphere.

Thus, the determination of atmospheric parameters with the API method shows that significant wave variations with periods of 5–10 min to several hours are regularly observed in the time dependences of the parameters of the lower ionosphere. The altitude profiles of the temperature and density of the neutral component, the velocity of vertical plasma motion, and different observation periods are characterized by a range of altitudinal variations from 5 km to 15–30 km.

5.2. Turbopause Height

A significant contribution to the dynamics of the mesosphere and lower thermosphere is made by turbulent movements of the neutral component. Turbulent formations are studied with many methods, which are selected based on the capabilities of the measuring equipment. These include the optical-rocket method for the measurement of the parameters of turbulence

and vertical wind velocity in the altitude range of 20–120 km (Andreeva L.A. et al., 1991), the radar method for the parameter measurement (Galedin et al., 1981; Kokin and Pakhomov, 1986), and vertical sounding of the ionosphere with the reception of signals backscattered by natural inhomogeneities of the ionospheric plasma (Schlegel K. et al., 1977).

The study of the mesosphere and lower thermosphere based on the creation and location of API makes it possible to determine some characteristics of atmospheric turbulence. As discussed above, as a result of its effect, artificial periodic irregularities in the E layer are destroyed (relax) faster than under the influence of ambipolar diffusion. The faster relaxation of irregularities begins at the turbopause level, the atmospheric height below which turbulent mixing predominates. Above it, the dominant process is ambipolar diffusion. Without dwelling in detail on the various definitions of the turbopause height (Tolmacheva et al., 2019), we will consider its height to be the level
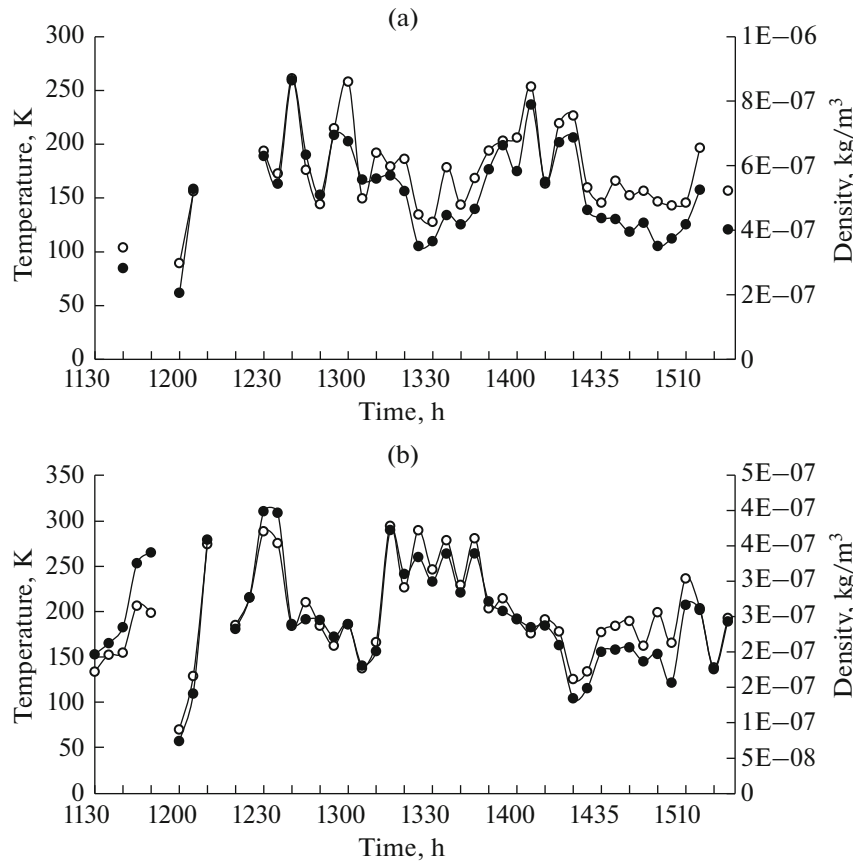
Fig. 9. Dependence of the temperature (circles) and density (points) of the neutral component on time on September 28, 2018, at an altitude of (a) 100 km and (b) 105 km . Pronounced wave movements with a period of 15 min to 2 h or more are clearly visible.

h_t at which turbulent diffusion begins to influence on the relaxation time of the scattered signal. In the example shown in Fig. 1, the effect of turbulence begins below 100 km and, obviously, the turbopause level is near this altitude.

Tolmacheva et al. (2019) analyzed in detail the results of measurements of the relaxation time of the scattered signal in the experiments performed mainly in the spring and autumn seasons of 2006–2015 and presented the results of the determination of the turbopause height. It was concluded that the average level of turbopause h_t amounted to 99–102 km with a tendency to decrease to 94 km in the evening in the autumn seasons at the latitude of the SURA stand. In general, the turbopause level varied in the altitude range of 94–106 km with periods from 10–15 to 30–40 min, which is naturally associated with the propagation of IGWs at these altitudes, as well as with their generation due to the development of convective instabilities (Tolmacheva et al., 2013). Under the conditions of developed convective instability, the region with turbulence can increase to 110 km with a significant increase in the temperature of neutrals. These findings (Tolmacheva et al., 2019) are confirmed by the results of experiments performed at the SURA

facility in 2015–2018. Figures 11a and 11b present examples of temporary variations in turbopause height h_t according to observations in the afternoon on September 28, 2018, and September 27, 2017. Each point in Fig. 11 corresponds to the averaged relaxation time over an interval of 5 min. The turbopause height h_t is located in the interval 91–101 km in the first case and in the interval 91–107 km in the second. Common in the changing magnitude h_t these days is its variability over time and the oscillatory nature of the variations. In Figure 11b, the interval of changes in the height of the turbopause expands to the region of large values. Note that, under conditions that are similar in geomagnetic and solar activity on days close to the autumn equinox, the nature of the time variation in the turbopause level is different. Particularly interesting in this connection is the example shown in Fig. 11b, which shows that the turbopause level is experiencing increasing amplitude and depth oscillations with a predominant period of 15–25 min. Similar increasing temperature fluctuations of the same periods are visible in Fig. 7b, which gives an example of neutral temperature variations with time. Thus, there is a definite correlation of variations in temperature and the turbopause level, the nature of which remains to be determined.
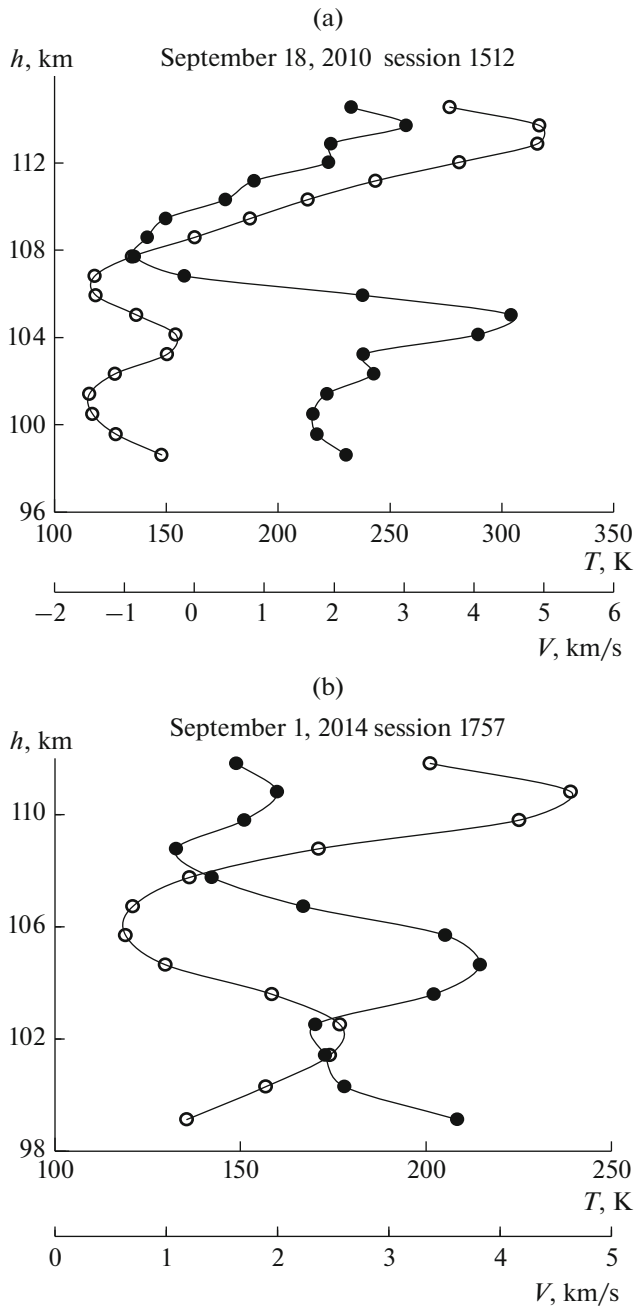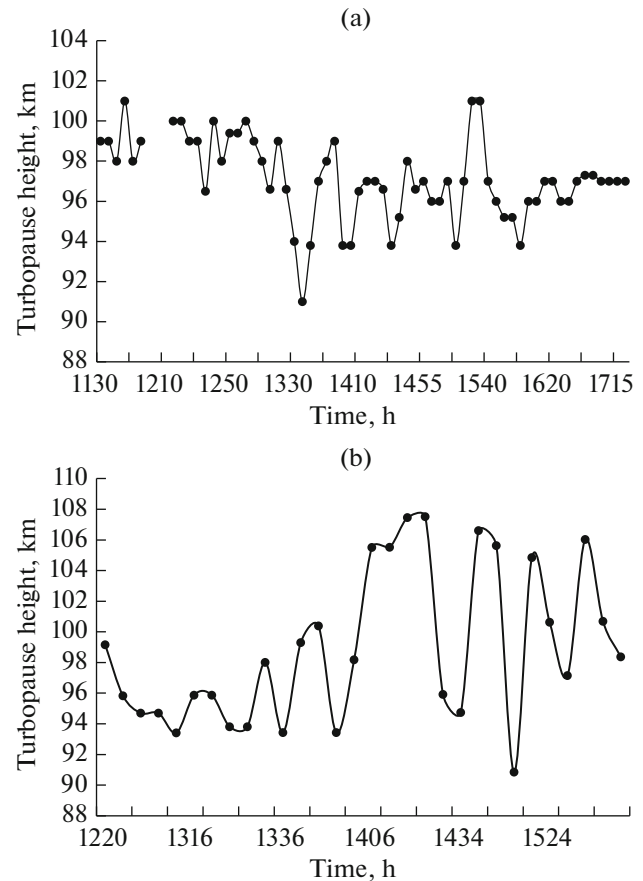
Fig. 10. Examples of altitude temperature profiles (points) and vertical velocity V (circles), changing (a) in phase and (b) in antiphase.

Fig. 11. Dependence of turbopause height on time according to observations in the afternoon on (a) September 28, 2018, and (b) September 27, 2017.

5.3. Turbulent Velocity

A reduction of the relaxation time relative to the time of the diffusion spreading of irregularities allows to be determined the vertical component of the turbulent velocity to be determined up to the height of the turbopause, near which the turbulent velocity approaches zero.

Since the velocity of turbulent movements V_t is determined by the deviation of the experimental altitude dependence $\tau(h)$ from diffusional, temporal vari-

ations V_t and $\tau(h)$ have similar features. The relaxation time and, accordingly, the turbulent velocity are subject to rapid fluctuations with a characteristic time of 15 s. Strong variations in $\tau(t)$ that do not fit into the framework of measurement errors, sometimes reflect the processes actually occurring at these heights. Variations in the turbulent velocity also exhibit rapid fluctuations and wave-like changes in time; therefore, it is usually determined from averaged relaxation times with an averaging interval of 1 to 15 min. The experiments conducted in different years showed that the minute values of V_t generally varied from values close to zero to 5 m/s (Bakhmeteva et al., 1996; Belikovich et al., 1999; Belikovich et al., 2002). In disturbed periods (wave phenomena, highly developed turbulence), the velocity V_t increased to 7 m/s. The average velocity of turbulent movements for a session lasting 6−7 h at altitudes below the turbopause was usually $V_t \approx 1-2$ m/s and decreased with height to values close to zero. Obviously, this height can be considered the turbopause height h_t. There was often a significant increase in V_t in the morning and a small increase in the afternoon, and the smallest were the velocity values near the local

noon. Fast turbulent velocity variations are shown in Fig. 12, which gives an example of its changes in time at an altitude of 100 km for observations on August 12, 1999 (the day after a single solar eclipse). The circles show the velocity values obtained with an interval of 15 s, and the dots and the curve show the values smoothed by the moving average method over a 5-min time interval. The example gives an idea of the depth and nature of fluctuations of turbulent velocity. Its variations are visible with periods from 10 to 90 min and a range of oscillations from 0.5 to 5 m/s. Note that such large V_t fluctuations indicate that the turbulence in the scattering volume manifests itself as an unsteady, random process. The correlation of minute (average per minute) changes in turbulent velocity at different heights is high in some cases, e.g., the correlation coefficient reached 0.9 at altitudes of 97 and 101 km by February 27, 1991 (Bakhmet'eva et al., 1996). In a number of sessions, there was a high correlation of turbulent velocity V_t at an altitude of 97 km and the velocity of vertical movement V at an altitude of 101 km, which may indicate turbulence intermittency, i.e., the "throwing" of regions with developed turbulence to large heights by large-scale vertical movements. One of the causes of atmospheric turbulence is its excitation by IGWs (Hines, 1975; Brunelli and Namgaladze, 1988; Fritts and Alexander, 2003), which is reflected in the oscillatory nature of turbulent velocity variations.

The sporadic E layer (E_s) is a process that competes with turbulence, which affects API formation and the characteristics of the scattered signal. This, conversely, causes an increase in the relaxation time at the height of the layer (Figs. 1 and 2b), which is due to the proportionality of the relaxation time of the scattered signal and the ion mass. Since the E_s layer contains atomic positive metal ions, including heavy ions of iron, magnesium, calcium, the average mass of ions at the heights of the E_s layer increases, which leads to an increase in the relaxation time and an increase in the amplitude of the scattered signal due to an increase in the reflection coefficient from the layer of probe radio waves. This fact was repeatedly noted in experiments on API observation, which allowed us to develop a method to determine the mass, i.e., the type of predominant ions in the sporadic E layer (Bakhmeteva et al., 2005; Bakhmeteva et al., 2010a).

6. ATMOSPHERIC WAVE PARAMETERS

The results of many years of experiments on the ionosphere at the SURA bench with the API method show that oscillatory motions of various periods are constantly present in temporal variations in the relaxation time of the scattered signal, the parameters of the neutral atmosphere (temperature, density, turbulent velocity, turbopause height), and the velocity of vertical plasma motion. Fluctuations with a period of more
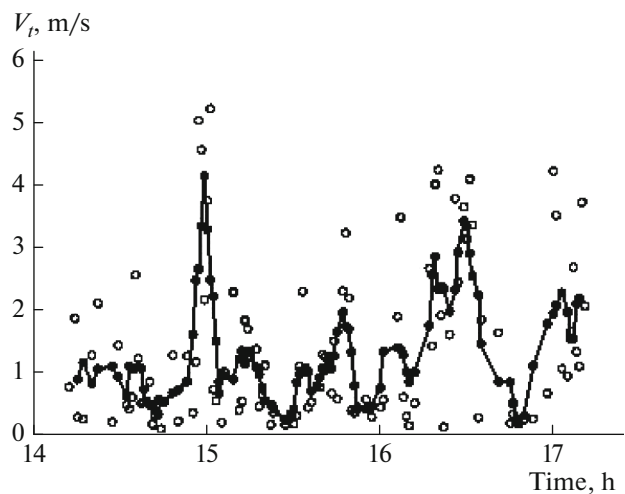
Fig. 12. Dependence of turbulent velocity V_t on time at an altitude of 100 km on August 12, 1999. The points correspond to signal registration every 15 s, and the curve corresponds to data smoothed by the moving average method over a 5-min interval.

than 5 min are usually interpreted as a result of IGW propagation (Hines, 1975; Gossard and Hook, 1978; Brunelli and Namgaladze, 1988; Grigoriev, 1999; Fritts and Alexander, 2002). The most pronounced wave movements are manifested in the time−altitude dependences of the velocity of vertical movement. As a rule, velocity changes direction; the velocity modulus usually grows with height. With increasing height, the amplitude of wave motions increases, sometimes reaching 12−15 m/s and contributing to variations in vertical velocity. Belikovich et al. (1999, 2002) presented data on the delay in wave oscillations $V(t)$ with increasing height, which corresponds to the downward-directed vertical component of the phase velocity with values of about 60−100 m/s; this is practically independent of the wave period. The vertical wavelengths are determined by altitude profiles $V(h)$, which lie in the interval from 3−5 km to 30 km. The wave spectra are a power-law function of frequency with an index on the order of 1 and a sharp kink near the Brant−Väisälä frequency (the eigenfrequency of the air element in the vertical direction), which makes it possible to determine this frequency experimentally. According to the spectral analysis of vertical velocity variations in different measurement periods, the periods of wave motions with a duration of 5−10, 15, 20, 30−40, and 60 min were reliably identified. On separate days of especially long measurements, intense wave motions with periods of 1.5, 2−2.5, 3.3, or more than 4 h were observed.

The influence of atmospheric waves on the development of environment instabilities in the lower ionosphere is analyzed based on the time−altitude dependences of the parameters of the neutral component (Bakhmeteva et al., 2002; Bakhmeteva et al., 2010b;

Tolmacheva et al., 2013). In many cases, perturbations of these parameters are observed, often with an unstable character that distorts their altitude profiles. These features were explained by the effect of IGW propagation and violation of the hydrodynamic stability of the medium. (Bahmeteva et al., 2002; Bakhmeteva et al., 2010; Tolmacheva et al., 2013). The application of the criteria for the development of medium instabilities to the development of time-altitude variations in atmospheric parameters, in comparison with the characteristics of wave and turbulent movements obtained in experiments, confirm the conclusion that instabilities and atmospheric waves have a significant effect on the dynamics of the mesosphere and the lower thermosphere in the altitude range 90−120 km.

7. CONCLUSIONS

The paper presents the results of a study of the dynamics of the Earth's mesosphere and lower thermosphere based on an analysis of the altitude−time variations of the parameters of the neutral component and the vertical velocity obtained by the method of resonant scattering of radio waves by artificial periodic irregularities of the ionospheric plasma. The temperature and density of the neutral component, the turbopause height, and the velocity of turbulent movements, as well as the velocity of the vertical regular plasma motion, were determined from measurements of the amplitude and phase of the signal scattered by irregularities. The high temporal resolution of the used method made it possible to identify rapid temporal variations in the parameters as one of the main special dynamics of the mesosphere and lower thermosphere, including a change in the magnitude and direction of the vertical velocity during one measurement over a period of 15 s. In most cases, a change in the velocity direction corresponds to the height of the sporadic E-layer maximum. The velocity values, as compared with atmospheric circulation models, indicate a significant influence of atmospheric waves. The time−altitude variations in the parameters of the neutral component convincingly demonstrated the significant effect of wave processes on them. Changes in time occur with a frequency characteristic of IGWs. The wave amplitude can reach 50 K or more in temperature variations and up to 12−15 m/s in vertical velocity. The greatest parameter variation takes place during solar eclipses and at sunset−sunrise hours due to the passage of "terminator" waves through the observation point. The altitude profile of the amplitude and relaxation time is influenced by mesospheric−thermospheric turbulence. The turbulent velocity of the medium is determined below the turbopause height, which reaches several m/s in some cases. In the autumn months, the turbopause level is in the altitude range of 90−108 km.

REFERENCES

Andreeva, L.A., Klyuev, O.F., Portnyagin, Yu.I., and Khanan'yan, A.A., *Issledovanie protsessov v verkhnei atmosfere metodom iskusstvennykh oblakov* (Study of Upper Atmospheric Processes by the Artificial Cloud Method), Leningrad: Gidrometeoizdat, 1991.

Bakhmet'eva, N.V., Belikovich, V.V., Benediktov, E.A., Bubukina, V.N., Goncharov, N.P., and Ignat'ev, Yu.A., Seasonal and diurnal variations of vertical motion velocities within mesosphere and lower thermosphere near Nizhnii Novgorod, *Geomagn. Aeron. (Engl. Transl.)*, 1996a, vol. 36, no. 5, pp. 675−681.

Bakhmet'eva, N.V., Belikovich, V.V., and Korotina, G.S., Determination of Turbulent Velocities with the Use of Artificial Periodic Inhomogeneities, *Geomagn. Aeron. (Engl. Transl.)*, 1996b, vol. 36, no. 5, pp. 724−726.

Bakhmet'eva, N.V., Belikovich, V.V., Grigor'ev, G.I., and Tolmacheva, A.V., Effect of acoustic gravity waves on variations in the lower-ionosphere parameters as observed using artificial periodic inhomogeneities, *Radiophys. Quantum Electron.*, 2002, vol. 45, no. 3, pp. 233−242.

Bakhmet'eva, N.V., Belikovich, V.V., Kagan, L.M., and Ponyatov, A.A., Sunset−sunrise characteristics of sporadic layers of ionization in the lower ionosphere observed by the method of resonance scattering of radio waves from artificial periodic inhomogeneities of the ionospheric plasma, *Radiophys. Quantum Electron.*, 2005, vol. 48, no. 1, pp. 14−28.

Bakhmet'eva, N.V., Belikovich, V.V., Bubukina, V.N., Vyakhirev, V.D., Kalinina, E.E., Komrakov, G.P., and Tolmacheva, A.V., Results of determining the electron number density in the ionospheric *E* region from relaxation times of artificial periodic irregularities of different scales, *Radiophys. Quantum Electron.*, 2008, vol. 51, no. 6, pp. 431−437.

Bakhmet'eva, N.V., Belikovich, V.V., Egerev, M.N., and Tolmacheva, A.V. Artificial periodic irregularities, wave phenomena in the lower ionosphere and the sporadic *E*-layer, *Radiophys. Quantum Electron.*, 2010a, vol. 53, no. 9, pp. 77−90.

Bakhmet'eva, N.V., Grigor'ev, G.I., and Tolmacheva, A.V., Artificial periodic irregularities, hydrodynamic instabilities, and dynamic processes in the mesosphere−lower thermosphere, *Radiophys. Quantum Electron.*, 2010b, vol. 53, no. 11, pp. 623−637.

Bakhmetieva, N.V., Bubukina, V.N., Vyakhirev, V.D., Grigoriev, G.I., Kalinina, E.A., and Tolmacheva, A.V., The results of comparison of vertical motion velocity and neutral atmosphere temperature at the lower thermosphere heights, *Proc. 5th Int. Conf. Atmosphere, Ionosphere, Safety,* Kaliningrad, 2016, pp. 197−202.

Bakhmet'eva, N.V., Vyakhirev, V.D., Kalinina, E.E., and Komrakov, G.P., Earth's lower ionosphere during partial solar eclipses according to observations near

Nizhny Novgorod, *Geomagn. Aeron. (Engl. Transl.)*, 2017a, vol. 57, no. 1, pp. 58−71.

Bakhmetieva, N.V., Bubukina, V.N., Vyakhirev, V.D., Grigoriev, G.I., Kalinina, E.E., and Tolmacheva, A.V., The results of comparison of vertical motion velocity and neutral atmosphere temperature at the lower thermosphere heights, *Russ. J. Phys. Chem. B.*, 2017b, vol. 11, no. 6, pp. 1017−1023.

Bakhmet'eva, N.V., Bubukina, V.N., Vyakhirev, V.D., Kalinina, E.E., and Komrakov, G.P., Response of the lower ionosphere to the partial solar eclipses of August 1, 2008 and March 20, 2015 based on observations of radio-wave scattering by the ionospheric plasma irregularities, *Radiophys. Quantum Electron.*, 2017c, vol. 59, no. 10, pp. 782−793.

Bakhmet'eva, N.V., Grigoriev, G.I., Tolmacheva, A.V., and Kalinina, E.E., Atmospheric turbulence and internal gravity waves examined by the method of artificial periodic irregularities, *Russ. J. Phys. Chem. B.*, 2018, vol. 12, no. 3, pp. 510−521.

Belikovich, V.V. and Benediktov, E.A., Influence of atmospheric turbulence on the relaxation of a signal scattered by artificial periodic inhomogeneities, *Geomagn. Aeron.*, 1995, vol. 35, no. 2, pp. 91−99.

Belikovich, V.V., Benediktov, E.A., Tolmacheva, A.V., and Bakhmet'eva, N.V., *Issledovanie ionosfery s pomoshch'yu iskusstvennykh periodicheskikh neodnorodnostei* (Study of the Ionosphere using Artificial Periodic Inhomogeneities), N. Novgorod: IPF RAN, 1999.

Belikovich, V.V., Benediktov, E.A., Tolmacheva, A.V., and Bakhmet'eva, N.V., *Ionospheric Research Using Artificial Periodic Irregularities*, Katlenburg-Lindau, Germany: Copernicus, 2002.

Belikovich, V.V., Bakhmet'eva, N.V., Kalinina, E.E., and Tolmacheva, A.V., A new method for determination of the electron number density in the *E* region of the ionosphere from relaxation times of artificial periodic inhomogeneities, *Radiophys. Quantum Electron.*, 2006, vol. 49, no. 9, pp. 699−674.

Borchevkina, O.P. and Karpov, I.V., Observations of variations in total electron content in the solar terminator region in the ionosphere, *Sovrem. Probl. Distantsionnogo Zondirovaniya Zemli Kosmosa*, 2018, vol. 15, no. 1, pp. 299−305.

Bryunelli, B.E. and Namgaladze, A.A., *Fizika ionosfery* (Physics of the Ionosphere), Moscow: Nauka, 1988.

Danilov, A.D., Kalgin, U.A., and Pokhunkov, A.A., Variation of the turbopause level in the polar regions, *Space Res.*, 1979, vol. 19, no. 83, pp. 173−176.

Fritts, D.C. and Alexander, M.J., Gravity waves dynamics and effects in the middle atmosphere, *Rev. Geophys.*, 2003, vol. 41, no. 1.
https://doi.org/10.1029/2001RG000106

Galedin, I.F., Neelov, I.O., and Pakhomov, S.V., Estimates for turbulent diffusivity in the mesosphere obtained by the radiolocation method, *Tr. Tsentr. Astrofiz. Obs.*, 1981, no. 144, pp. 22−27.

Gershman, B.N., *Dinamika ionosfernoi plazmy* (Dynamics of Atmospheric Plasma), Moscow: Nauka, 1974.

Gershman, B.N., Ignat'ev, Yu.A., and Kamenetskaya, G.Kh., *Mekhanizmy obrazovaniya sporadicheskogo sloya E_s na raznykh shirotakh* (Mechanisms of the Formation of the Sporadic Layer E_s at Various Latitudes), Moscow: Nauka, 1976.

Gossard, E.E. and Hook, W.H., *Waves in the Atmosphere*, Amsterdam: Elsevier, 1975; Moscow: Mir, 1978.

Grigor'ev, G.I., Acoustic−gravity waves in the Earth's atmosphere (review), *Radiophys. Quantum Electron.*, 1999, vol. 42, no. 1, pp. 1−21.

Haines, K.O., Atmospheric gravity waves, *Thermospheric Circulation*, Webb, W.L., Ed., Cambridge: MIT, 1972; Moscow: Mir, 1975, pp. 85−99.

Hocking, W.K., Dynamical coupling processes between the middle atmosphere and lower ionosphere, *J. Atmos. Terr. Phys.*, 1996, vol. 58, no. 6, pp. 735−752.

Izmerenie vetra na vysotakh 90−100 km nazemnymi metodami (Measurements at Altitudes of 90−100 km by Ground-Based Methods), Portnyagin, Yu.I. and Sprenger, K., Eds., Leningrad: Gidrometeoizdat, 1978.

Kagan, L.M., Bakhmet'eva, N.V., Belikovich, V.V., and Tolmacheva, A.V., Structure and dynamics of sporadic layers of ionization in the ionospheric e region, *Radio Sci.*, 2002, vol. 37, no. 6, pp. 1106−1123.

Kalgin, Yu.A. and Danilov, A.D., Determination of eddy diffusivity parameters in the mesosphere and lower thermosphere, *Geomagn. Aeron.*, 1993, vol. 33, no. 6, pp. 119−125.

Karimov, K.A., *Vnutrennie gravitatsionnye volny v verkhnei atmosfere* (Internal Gravity Waves in the Upper Atmosphere), Frunze: Ilim, 1983.

Karpov, I.V. and Kshevetskii, S.P., Formation of large-scale disturbances in the upper atmosphere caused by acoustic gravity wave sources on the Earth's surface, *Geomagn. Aeron. (Engl. Transl.)*, 2014, vol. 54, no. 4, pp. 513−522.

Karpov, I.V., Kshevetskii, S.P., Borchevkina, O.P., Radievskii, A.V., and Karpov, A.I., Disturbances of the upper atmosphere and ionosphere caused by acoustic-gravity wave sources in the lower atmosphere, *Russ. J. Phys. Chem. B*, 2016, vol. 35, no. 1, pp. 127−132.

Khanan'yan, A.A., The vertical structure of wind and turbulence in the lower thermosphere of midlatitudes, *Issledovanie dinamicheskikh protsessov v verkhnei atmosfer* (Study of Dynamical Processes in the Upper Atmosphere), Lysenko, I.A., Ed., Moscow: Gidrometeoizdat, 1985, pp. 59−63.

Kirkwood, S., Seasonal and tidal variations of neutral temperatures and densities in the high latitude lower thermosphere measured by EISCAT, *J. Atmos. Terr. Phys.*, 1996, vol. 58, no. 6, pp. 735−752.

Kokin, G.A. and Pakhomov, S.V., The turbulent regime of region D in the winter of 1983−1984, *Geomagn. Aeron.*, 1986, vol. 26, no. 5, pp. 714−717.

Mathews, J.D., Sporadic E: Current views and recent progress, *J. Atmos. Sol.-Terr. Phys.*, 1998, vol. 60, no. 4, pp. 413−435.

Medvedeva, I.V. and Ratovsky, K.G., Comparative analysis of atmospheric and ionospheric variability by measurements of temperature in the mesopause region and peak electron density *NmF*2, *Geomagn. Aeron. (Engl. Transl.)*, 2017, vol. 57, no. 2, pp. 217−228.

Offermann, D., Jarisch, M., Oberheide, J., Gusev, O., Wohltmann, I., Russel, III J.M., and Mlynczak, M.G., Global wave activity from upper stratosphere to lower

thermosphere: A new turbopause concept, *J. Atmos. Sol.−Terr. Phys.*, 2006, vol. 68, no. 15, pp. 1709−1729.

Perminov, V.I., Semenov, A.I., Medvedeva, I.V., and Pertsev, N.N., Temperature variations in the mesopause region according to the hydroxyl-emission observations at midlatitudes, *Geomagn. Aeron. (Engl. Transl.)*, 2014, vol. 54, no. 2, pp. 230−239.

Schlegel, K., Brekke, A., and Haug, A., Some characteristics of the quiet polar D-region and mesosphere obtained with the partial reflection method, *J. Atmos. Terr. Phys.*, 1977, vol. 40, no. 2, pp. 205−213.

Somsikov, V.M., Solar terminator and dynamic phenomena in the atmosphere: A review, *Geomagn. Aeron. (Engl. Transl.)*, 2011, vol. 51, no. 6, pp. 707−719.

Tolmacheva, A.V., Grigoriev, G.I., and Bakhmetieva, N.V., The variations of the atmospheric parameters on measurements using the artificial periodic irregularities of plasma, *Russ. J. Phys. Chem. B*, 2013, vol. 7, no. 5, pp. 663−669.

Tolmacheva, A.V., Bakhmetieva, N.V., Grigoriev, G.I., and Kalinina, E.E., The main results of the long-term measurements of the neutral atmosphere parameters by the artificial periodic irregularities techniques, *Adv. Space Res.*, 2015, vol. 56, no. 6, pp. 1185−1193.

Tolmacheva, A.V., Bakhmetieva, N.V., Grigoriev, G.I., and Egerev, M.N., Turbopause range measured by the method of the artificial periodic irregularities, *Adv. Space Res.*, 2019, vol. 64, no. 10, pp. 1968−1974.

Vlasov, M.N. and Kelley, M.C., Specific features of eddy turbulence in the turbopause region, *Ann. Geophys.*, 2014, vol. 32, pp. 431−442.

Whitehead, J.D., Recent work on mid-latitude and equatorial sporadic-E, *J. Atmos. Terr. Phys.*, 1989, vol. 51, no. 5, pp. 401−424.